# Ultrafast electronic band gap control in an excitonic insulator

**Selene Mor**[1], **Marc Herzog**[1], **Denis Golež**[2], **Philipp Werner**[2], **Martin Eckstein**[3], **Naoyuki Katayama**[4], **Minoru Nohara**[5], **Hide Takagi**[6,7], **Takashi Mizokawa**[8], **Claude Monney**[9,*], and **Julia Stähler**[1]

[1] Dept. of Physical Chemistry, Fritz-Haber-Institut der Max-Planck-Gesellschaft, 14195 Berlin, Germany

[2] Dept. of Physics, Univ. of Fribourg, 1700 Fribourg, Switzerland

[3] Max Planck Research Department for Structural Dynamics, Univ. of Hamburg-CFEL, 22761 Hamburg, Germany

[4] Dept. of Physical Science and Engineering, Nagoya Univ., 464-8603 Nagoya, Japan

[5] Research Institute for Interdisciplinary Science, Okayama University, Okayama 700-8530, Japan

[6] Max Planck Institute for Solid State Research, 70569 Stuttgart, Germany

[7] Dept. of Physics, Univ. of Tokyo, 113-8654 Tokyo, Japan

[8] Dept. of Applied Physics, Waseda Univ., 169-8555 Tokyo, Japan

[9] Dept. of Physics, Univ. of Zurich, 8057 Zurich, Switzerland

[*] monney@physik.uzh.ch

**ABSTRACT**

Symmetry-broken states are characterized by an order parameter, which usually appears if a material is cooled below a critical temperature. These fragile states are typically destroyed by strong optical pulses on an ultrafast timescale. A nontrivial challenge is therefore the *enhancement* of an order parameter by optical excitations, as this implies a strengthening of long-range order in a perturbed system. Here, we investigate the non-equilibrium dynamics of the electronic structure of the layered semiconductor $Ta_2NiSe_5$ using time- and angle-resolved photoelectron spectroscopy. We show that below the critical excitation density of $F_C = 0.2$ mJ cm$^{-2}$, the direct band gap is transiently *reduced*, while it is *enhanced* above $F_C$. An analysis based on Hartree-Fock calculations reveals that this intriguing effect can be explained by the exotic low-temperature ordered state of $Ta_2NiSe_5$, which hosts an exciton condensate whose order parameter is connected to the gap size. These results demonstrate the ability to manipulate condensates of bound electron-hole pairs with light, and due to the similarity to BCS theory, this approach might also be applicable to the case of superconductors.

## Main text

Semiconductor materials are intensively studied due to their technological importance, for instance in the field of photovoltaics or data processing. The elementary excitation of a semiconductor is the transfer of an electron across the semiconductor band gap $E_g$ from the fully occupied valence band (VB) to the unoccupied conduction band (CB), leaving a hole behind. The free carriers and charge redistributions generated, for instance, by light absorption modify the screening properties and electrostatic (Hartree) energies, which may lead to a shifting of the CB and VB toward each other and hence a narrowing of the band gap. This process is referred to as band gap renormalization.[1–8] In addition, due to the attractive Coulomb interaction (CIA) between the oppositely charged carriers, bound electron-hole pairs, called excitons, may form after the relaxation of the electrons and holes toward the band extrema. Such excitons usually have a finite lifetime, depending on the recombination probability and availability of dissociation channels.[9]

When, for example in small gap semiconductors with low dielectric constant, the electron and hole are so strongly bound that the exciton binding energy $E_B$ exceeds the band gap $E_g$, a new situation arises (see fig. 1(b)). Then, the spontaneous formation of excitons, without any external stimulus, results in

a total energy gain. Similar to Bose-Einstein condensation in, for example, superfluid $He_4$,[10] or BCS superconductivity,[11] a macroscopic condensation of excitons has been predicted to occur in small gap semiconductors, resulting in a new ground state, the excitonic insulator (EI) phase.[12–14] This EI phase is characterized by a wider band gap $E_g + 2\Delta$, where $\Delta$ is the energy difference between the parabolic (semiconductor) and flat upper (excitonic insulator) VB maxima, which is related to the exciton condensate density and hence to the order parameter of the phase transition.[12]

In the past, it has been difficult to address exciton condensates experimentally, as excitons, usually, have finite lifetimes and low binding energies that limit the build-up of a condensate. However, these difficulties have been circumvented by, for instance, coupled quantum wells where exciton lifetimes are enhanced through spatial separation.[15–19] Complementary to these studies of (meta)stable realizations of EIs, a few materials have been suggested to exhibit a *ground state* EI phase, like $Ta_2NiSe_5$ (TNS)[20,][21] $TiSe_2$[22,23] , and $TmSe_{0.45}Te_{0.55}$[24,25] where $E_B > E_g$ and exciton formation and condensation is considered to occur spontaneously.

The quasi-one dimensional TNS shows a second-order phase transition at a critical temperature of $T_C = 328$ K, accompanied by a structural distortion.[20,26] Above $T_C$, TNS exhibits a direct band gap at $\Gamma$, which increases[27] up to approximatively 0.3 eV with decreasing the temperature[28] below $T_C$. Simultaneously, an anomalous flattening and broadening of the VB occurs which has been interpreted as a signature of the formation of an EI phase in TNS.[20,21,28,29] Contrary to the indirect band gap material $TiSe_2$, the EI phase of TNS is not coupled to a charge density wave.[30,31] It, thus, offers the unprecedented opportunity to directly investigate the effect of photoexcitation between the electronic states involved in the exciton formation, without the complication of a charge density wave.[32,33]

Not much is known about the *non-equilibrium* properties of exciton condensates, although these are crucial with regard to any potential application, which naturally occurs out of equilibrium. Envisioning the optical control of an exciton condensate and thus the material's band gap, or even imagining the manipulation of other Bose-Einstein condensates to achieve, for example, photoinduced superconductivity on ultrafast timescales, requires sound understanding of the elementary processes following optical excitation of the condensate. In particular, what is the impact of free carrier screening on the band gap and does it matter which bands are populated directly by the photoexcitation? Can the exciton density and

therefore the order parameter be enhanced by light absorption? Can these transient properties be tuned by tailouring the optical excitation to achieve full control of a material band gap?

Towards these aims, we study here the ultrafast, non-equilibrium dynamics of the occupied electronic structure of TNS using time- and angle-resolved photoelectron spectroscopy (trARPES). We show that, at modest near-infrared (NIR) excitation densities ($< F_C = 0.2$ mJ cm$^{-2}$), the occupied electronic structure exhibits an abrupt shift towards the Fermi energy, $E_F$. These dynamics are indicative of a transient narrowing of the band gap induced by free-carrier screening of the CIA and Hartree shifts. Above $F_C$, however, the direct band gap of TNS is transiently *enhanced* on the timescale of 200 fs. As this behavior is opposite to that of ordinary semiconductors, we argue, on the basis of Hartree-Fock calculations, that it is a direct consequence of the transient enhancement of the order parameter of the exciton condensate. We demonstrate that we can either increase or decrease the size of the band gap in the semiconductor TNS by tuning the NIR excitation density, the proof of principle of ultrafast electronic band gap control in a semiconductor.

The electronic structure of TNS and the experimental scheme[34] are illustrated in fig. 1(a). From the upper VB, two electronic transitions can be optically excited by an ultrashort NIR laser pulse with a photon energy of h$\nu_{pump} = 1.55$ eV: (1) to the flat unoccupied $d$-band at $\Gamma$ (i.e. $k = 0$), and (2) to the lowest CB, but at larger $k$-vectors. The occupied electronic band structure and its non-equilibrium dynamics are monitored by ARPES of the blue shaded region using h$\nu_{probe} = 6.2$ eV.

At $T = 110$ K and in equilibrium, i.e. without pump excitation, TNS exhibits, as shown in fig. 1(c), two occupied VBs with maxima at $E - E_F \approx -0.5$ eV and $-0.1$ eV, respectively, which is consistent with previous ARPES results.[20] Considering the optical gap of 0.3 eV, the sample appears to be slightly p-doped. Fig. 1(d) shows the temporal evolution of the photoelectron (PE) intensity at $\Gamma$ and $T = 110$ K in false color representation after moderate photoexcitation. The data reveal a rapid response to the optical excitation at $t = 0$ fs: a massive suppression of PE intensity within the first 500 fs, and an energy shift of both VBs towards $E_F$. This is further illustrated by two energy distribution curves (EDCs), before (empty grey circles) and 190 fs after (solid red circles) NIR photoexcitation in fig. 1(e). For a quantitative analysis of the monitored electronic structure dynamics, we fit such EDCs at various pump-probe time delays[34] and obtain the transient amplitude of the spectral function and energetic position at $\Gamma$ for each

band. Two exemplary fits are shown in fig 1(e) (solid lines). The resulting peak positions are depicted in panel (d) (red circles), confirming that both VBs show an abrupt upward shift upon photoexcitation, which is more pronounced for the lower band.

Fig. 1(f) displays the temporal evolution of the flat top VB amplitude at $\Gamma$ for different incident pump fluences: the VB is increasingly depopulated by the increasing excitation density and its occupation recovers, on average, within $870 \pm 210$ fs [1]. The population minima scale linearly with the pump fluence up to a critical value $F_C \approx 0.2$ mJ cm$^{-2}$ above which the VB depopulation saturates at $\sim 50\%$, as shown in fig. 1(g). It seems likely that this behaviour results from an absorption saturation along the lines of Einstein's derivations for a two-level system.[35]

Before turning to a discussion of the transient shift of the flat top VB with respect to its equilibrium energetic position at the $\Gamma$-point ($k = 0$), we focus on the shifts observed for the upper VB at $k \neq 0$ and the lower VB at $k = 0$ shown in fig. 2. The latter are expected to remain largely unaffected by photoinduced changes to the exciton condensate. Different trace colors correspond to different excitation densities. In both cases, the bands shift abruptly toward lower binding energy, i.e. toward $E_F$. This upward shift is the fingerprint of a *transient shrinking* of the band gap following the photoexcitation. We quantify these dynamics by fitting a single exponential decay convoluted with the laser pulses' envelope[34] as exemplarily shown by the black curves in fig. 2. At all fluences and for both VBs, the peak shift recovers on comparable timescales below 1 ps. Clearly, this is in good agreement with the timescale observed for the population dynamics of the photoinduced carriers at $\Gamma$, see fig. 1(f). Furthermore, the band shift becomes stronger with increasing excitation density up to the same critical fluence $F_C$ at which the absorption saturation of the flat top VB occurs. These findings strongly suggest that the abrupt band gap narrowing is a consequence of the photocarriers generated by photoexcitation (1) from the flat top VB.

The photoinduced shift of the flat top VB at $\Gamma$ is shown in fig. 3(a). For $F < F_C$, the dynamics resemble the trend observed at $k \neq 0$ (see fig. 2(a)), although less pronounced at the respective fluences (blue to light green traces). The same fit function (solid black) as in fig. 2 is used to quantify these early dynamics. However, for larger fluences, we observe a shift in the *opposite* direction, delayed by $\sim 200$ fs,

---

[1] The change of the integral of the VB spectral function can be interpreted as a measure for its occupation evolution under the established assumption of temporally constant transfer matrix elements.

such that the flat top VB maximum transiently lies at *higher* binding energies than its equilibrium position (yellow and orange traces). After approximately 1 ps, this effect relaxes by an upward shift of the band that even "overshoots" the equilibrium position. The delayed downshift of the flat top VB is sufficiently pronounced to be directly seen in the raw PE data, as evidenced by the normalized EDCs in fig. 3(b) for different time delays before (empty grey circles) and after (solid red circles) photoexcitation. These results demonstrate that the band gap of TNS is transiently *enhanced* by strong photoexcitation.

Fig. 4(a) summarizes the observed different VB shifts at three points in the TNS electronic structure as a function of the incident fluence. Clearly, the upward shift occurring in the upper VB at $k \neq 0$ (yellow) and in the lower VB at $\Gamma$ (green) is enhanced with increasing excitation density and exhibits a slope change at the same critical fluence $F_C$ as the VB depopulation threshold shown in fig. 1(f). The transient shift of the flat top VB at $\Gamma$ follows, on the contrary, a non-monotonic curve, revealing that two competing phenomena are at play: While, for $F < F_C$, the flat top VB qualitatively follows the trend of the yellow and green curves, a *time-delayed* process counteracts this band gap narrowing for $F > F_C$. This is reflected in a shift away from $E_F$ with respect to the equilibrium position and, consequently, a transient widening of the band gap at $\Gamma$.

Both effects are illustrated by the insets in fig. 4(a). As the upward shift saturates at $F_C$, we conclude that it must be connected to the transient free carrier density that is generated by excitation mechanism (1) (cf. fig. 1(a)) where carriers from the flat top VB are transferred to the upper CB, a process that saturates at a population redistribution of 50 %. The upward shift is, thus, driven by a band gap renormalization which is caused by free carrier screening, as expected for a semiconductor under optical excitation.[1–8] Once excitation mechanism (1) has saturated, excitation (2), which occurs away from $\Gamma$ (cf. fig. 1(a)), becomes increasingly important. It seems plausible that this dominance of excitation (2), which takes place within the upper VB and lower CB, for $F > F_C$ is responsible for the sign change of the flat top VB shift at $\Gamma$. This extraordinary behavior is analyzed with regard to the presence of an exciton condensate in the following.

In particular we show that, in the presence of an exciton condensate, nonthermal carrier distributions and a decrease of the semiconductor band gap can lead to an enhancement of the condensate density and a corresponding enhancement of the band gap at $\Gamma$. To demonstrate this, we perform a Hartree-Fock

calculation for the simplified case of a one-dimensional two-band system, representing the upper VB and lower CB. The bands are shown in fig. 4(b), where the dashed (solid) curves represent the noninteracting (interacting) case. In order to mimic the effect of excitation mechanism (1) that involves also other bands in the experiment, we reduce the splitting between the bare semiconductor VB and CB by some value $\delta\eta$ (fig. 4(b)). The effect of excitation (2) is *explicitly* included in the calculation in the form of a nonthermal carrier distribution as shown in panel (c) (dark red). Clearly, we observe that the interplay of (1) and (2) can lead to an enhancement of the band gap at $\Gamma$ while the bands shift towards each other at larger $k$ (compare solid dark red and grey lines in fig. 4(b)) as observed in the experiment.

The enhancement of the gap in the Hartree-Fock calculation is related to an increase of the exciton condensate density (and hence of the order parameter of the EI phase), which relies on two effects: on the one hand, one finds that for a given value of the CIA the equilibrium condensate density increases if the (noninteracting) conduction and valence bands are shifted closer together, because then excitons are formed from more resonant states. The electrostatic effect of a photoexcited electron density $n_{ex}$ (i.e., the Hartree contribution to the interaction) can produce such a shift, and thus tends to enhance the density of condensed pairs. On the other hand, a large $n_{ex}$ weakens the condensate, similar to a thermal population of quasiparticle states. The crucial observation is that this potentially detrimental effect of the photoexcited population on the order parameter can be much weaker in a nonthermal state than in a thermal one: for the parameters of fig. 4(b) and an excitation density of $n_{ex} = 0.02$ we use the nonthermal carrier distribution displayed in panel (c) (dark red). In this situation the exciton condensate is enhanced. This enhancement of the order parameter in the presence of nonthermal quasiparticles is robust for a broad range of distribution functions, e.g., for a flat distribution, or one where electron and hole distributions are thermalised independently within the VB and CB, see fig. 4(f). For all these nonthermal distributions the band gap at $\Gamma$ is enhanced, once the CIA between electrons and holes is switched on (solid curves) and a Hartree shift is applied, while in the *fully* thermalized state the temperature would be above the melting temperature of the condensate. This means that photoexcitation of an EI can result in a transient enhancement of the order parameter, if thermalization is sufficiently delayed by, for instance, the presence of the band gap. On longer timescales, as thermalization occurs, we expect a band gap reduction, as is indeed observed in the experiments after about 1 ps (cf. fig. 3(a)).

To summarize, the discovery of a transient band gap enhancement in the layered semiconductor $Ta_2NiSe_5$ upon photoexcitation can be consistently explained by the existence of an excitonic insulator phase in this material. We propose that the strengthening of the condensate in the perturbed state is a consequence of the low-energy electronic structure of this material, which provides different channels for resonant excitation and the possibility of significant Hartree shifts and nonthermal quasiparticle distributions. Our results demonstrate that there exists a critical fluence of the photoexcitation separating regimes in which the semiconductor band gap can be either increased or decreased offering the possibility of controlling the band gap by tuning the photoexcitation fluence. Moreover, our study strongly suggests that photoexcitation at lower photon energies, which favours excitation mechanism (2), could be used to enhance the condensate density even further. Clearly, this will stimulate further experimental and theoretical investigations of this effect aimed at a complete characterization. Interestingly, the recent observation of the enhanchement of the charge density wave amplitude in elemental chromium[36] typifies another, very different possibility of enhancing order by photoexcitation. Furthermore, it seems possible to apply the demonstrated mechanism of manipulating quasiparticle condensates also to the case of BCS superconductors: in the vicinity of a van Hove singularity, a rigid band shift induced by the electrostatic potential of excited nonthermal carriers can strongly increase the electronic density of states at low energies, which might lead to a transient enhancement of the superconducting condensate density on ultrafast timescales.

## Methods

### Experimental details

TNS single crystalline samples were prepared by reacting the elementals nickel, tantalum and selenium with a small amount of iodine in a evacuated quartz tube. The tube was slowly heated and kept with a temperature gradient from 950 °C to 850 °C for 7 days, followed by slow cooling. Single crystalline samples with a typical size of 0.04 x 1 x 10 $mm^3$ were obtained in the cooler end.

For the photoemission experiments, the samples were cleaved *in situ* at room temperature under ultrahigh vacuum (UHV) conditions ($p = 1.6$ x $10^{-10}$ mbar) and then slowly cooled down to 110 K using liquid $N_2$. TNS was optically excited by the p-polarized, fundamental output (h$\nu_{pump}$ = 1.55 eV) of a

regeneratively amplified Ti:Sa laser system working at a repetition rate of 40 kHz. The photoinduced changes to the electronic structure along the Ni chain direction of TNS was probed by time-delayed p-polarized probe pulses ($h\nu_{\mathrm{probe}}$ = 6.2 eV), generated by frequency quadrupling of the fundamental. The photoemitted electrons were detected by a hemispherical analyzer (SPECS Phoibos 100) that was held at a bias voltage of 0.5 eV with respect to the sample holder. The energy resolution of 86 meV is obtained as root sum squared of the UV pulse bandwidth (25 meV) and the instrument resolution (82 meV) estimated *in situ* from the low-energy secondary electron cut-off of a direct photoemission spectrum of the metallic sample holder. PE spectra are plotted as a function of energy with respect to the equilibrium Fermi level $E - E_{\mathrm{F}} = E_{\mathrm{kin}} - h\nu_{\mathrm{probe}} + \Phi$. $\Phi$ is the work function. $E_{\mathrm{F}}$ was determined independently on the metallic sample holder, which was in direct electrical contact with the sample. We can neglect sample charging as the origin of the observed transient spectral shifts as (i) no *rigid* shift of the angle-resolved PE spectra was observed (parts of the spectrum shift up, others down) and (ii) the low-energy secondary electron cut-off remains unchanged. The energetic offset of the band positions in fig. 1(c) and (d, negative delays) is attributed to the heat-load of the pump pulse that is not fully dissipated within the repetition rate of the experiment.

EDCs were fitted with a sum of three Gaussian peaks multiplied by the Fermi-Dirac occupation distribution and convoluted with another Gaussian to account for the energy resolution. The Gaussian peak at lower binding energy is fit to the lower VB, while the sum of the other two Gaussians is used to reproduce the asymmetric shape of the upper VB. Different fit functions lead to qualitatively the same peak shifts, as the effects are sufficiently strong to be seen in the raw data (see fig. 3(b)). The energetic position of the maximum of this combined peak was used as a measure for the energetic position of the upper VB. The transient population of the VBs has been estimated from the area under the corresponding peak at each pump-probe delay.

The two-photon photoemission signal of TNS at high kinetic energies represents a cross correlation of the Gaussian pump and probe laser pulses and was used to estimate an upper limit for the time resolution of 110 fs.

## Theoretical modeling

We investigate the dynamics of the EI by considering a one-dimensional two-band system of spin-less fermions with direct band gap, $H = H_0 + H_{\text{int}}$, where the noninteracting part is

$$H_0 = \sum_{k,\alpha} (\varepsilon_{k,\alpha} + \eta_\alpha) c^\dagger_{k,\alpha} c_{k,\alpha},$$

with the band dispersion $\varepsilon_{k,1(2)} = -(+)2t_0 \cos(k)$. The $c_{k,\alpha}$ denote the annihilation operators for an electron with momentum $k$ in orbital $\alpha = 1, 2$. The bare band splittings $\eta_{1,2}$ are chosen such that band $1$ ($2$) is totally occupied (unoccupied). For the interaction we consider a local density-density CIA of the form

$$H_{\text{int}} = \frac{1}{2} \sum_i U n_{i,1} n_{i,2}.$$

The hopping parameter $t_0$ and interaction strength $U$ are chosen such that the ground state gap matches the experimental one. Explicitly, for the ground state calculations, we used $t_0 = 0.26$ eV, $U/t_0 = 3.0$ and the relative bare band splitting $(\eta_2 - \eta_1)/t_0 = 2.1$.

The excitonic instability arises because of the attractive CIA between the electrons in the upper band and the holes in the lower band, leading to a condensation of the excitons which are formed across the direct band gap. The order parameter of the condensate is $\rho_{12} = \langle c^\dagger_{k,1} c_{k,2} \rangle \neq 0$. In order to solve the problem we employ standard Hartree-Fock calculations based on the mean-field decoupling of the interaction term. The experimentally observed abrupt band gap narrowing is modeled by a reduction of the bare band splitting $\eta_2 - \eta_1$ between the VB and CB. The effect of the nonthermal distribution on the band gap size $\Delta$ is determined from the self-consistent Hartree-Fock calculation. In order to show that the conclusions do not depend on the particular choice of the distribution function, we compared several parametrizations of the nonthermal distribution function, see also fig.4(e)-(f): (i) additional constant population of holes (electrons), (ii) Lorentzian peak (dip) in the Fermi-Dirac distribution function below (above) $E_F$, namely $f_{\text{nth}}(\varepsilon, A, \overline{E}) = f_{\text{FD}}(\varepsilon, 0) + A\gamma^2 / ((\varepsilon - \overline{E})^2 + \gamma^2)$, where $f_{\text{FD}}(\varepsilon, \mu)$ is the Fermi-Dirac distribution, $A$ is the amplitude, $\gamma$ the width and $\overline{E}$ the center position of the Lorentzian peak (dip), (iii) intraband thermalized distributions at elevated temperatures.

# References

1. Berggren, K. F. & Sernelius, B. E. Band-gap narrowing in heavily doped many-valley semiconductors. *Phys. Rev. B* **24**, 1971–1986 (1981).

2. Oschlies, A., Godby, R. W. & Needs, R. J. First-principles self-energy calculations of carrier-induced band-gap narrowing in silicon. *Phys. Rev. B* **45**, 13741–13744 (1992).

3. Pagliara, S. *et al.* Photoinduced $\pi$-$\pi$* band gap renormalization in Graphite. *J. Am. Chem. Soc.* **133**, 6318–6322 (2011).

4. Chernikov, A., Ruppert, C., Hill, H. M., Rigosi, A. F. & Heinz, T. F. Population inversion and giant bandgap renormalization in atomically thin $WS_2$ layers. *Nature Photonics* **9**, 466–470 (2015).

5. Pogna, E. A. A. *et al.* Photo-induced bandgap renormalization governs the ultrafast response of single-layer $MoS_2$. *ACS Nano* **10**, 1182–1188 (2016).

6. Dou, Y., Fishlock, T., Egdell, R. G., Law, D. S. L. & Beamson, G. Band-gap shrinkage in n-type-doped CdO probed by photoemission spectroscopy. *Phys. Rev. B* **55**, R13381–R13384 (1997).

7. Wagner, J. Band-gap narrowing in heavily doped silicon at 20 and 300 K studied by photoluminescence. *Phys. Rev. B* **32**, 1323–1325 (1985).

8. Wegkamp, D. *et al.* Instantaneous band gap collapse in photoexcited monoclinic $VO_2$ due to photocarrier doping. *Phys. Rev. Lett.* **113**, 216401 (2014).

9. Münzhuber, F. *et al.* Exciton decay dynamics controlled by impurity occupation in strongly Mn-doped and partially compensated bulk GaAs. *Phys. Rev. B* **90**, 125203 (2014).

10. Kapitza, P. Viscosity of liquid helium below $\lambda$-point. *Nature* **141**, 3558 (1938).

11. Bardeen, J., Cooper, L. N. & Schrieffer, J. R. Theory of superconductivity. *Phys. Rev.* **108**, 1175 (1957).

12. Jérome, D., Rice, T. M., & Kohn, W. Excitonic insulator. *Rev. Mod. Phys.* **158**, 462 (1967).

13. Keldysh, L. V. & Kopaev, Y. V. Possible instability of semimetallic state toward coulomb interaction. *Sov. Phys. Solid State* **6**, 2219 (1965).

14. Zenker, B., Ihle, D., Bronold, F. X. & Fehske, H. Electron-hole pair condensation at the semimetal-semiconductor transition: A bcs-bec crossover scenario. *Phys. Rev. B* **85**, 121102(R) (2012).

15. Butov, L., Lai, C., Ivanov, A., Gossard, A. & Chemla, D. S. Towards Bose–Einstein condensation of excitons in potential traps. *Nature* **417**, 47–52 (2002).

16. Keeling, J., Levitov, L. S. & Littlewood, P. B. Angular distribution of photoluminescence as a probe of Bose condensation of trapped excitons. *Phys. Rev. Lett.* **92**, 176402 (2004).

17. Eisenstein, J. & MacDonald, A. Bose–Einstein condensation of excitons in bilayer electron systems. *Nature* **432**, 691–694 (2004).

18. Snoke, D. Condensed-matter physics: coherent questions. *Nature* **443**, 403 (2006).

19. Snoke, D. Spontaneous Bose coherence of excitons and polaritons. *Science* **298**, 1368–1372 (2002).

20. Wakisaka, Y. *et al.* Excitonic insulator state in $Ta_2NiSe_5$ probed by photoemission spectroscopy. *Phys. Rev. Lett.* **103**, 026402 (2009).

21. Seki, K. *et al.* Excitonic bose-einstein condensation in $Ta_2NiSe_5$ above room temperature. *Phys. Rev. B* **90**, 155116 (2014).

22. Cercellier, H. *et al.* Evidence for an excitonic insulator phase in $1T$-$TiSe_2$. *Phys. Rev. Lett.* **99**, 146403 (2007).

23. Monney, C., Monney, G., Aebi, P. & Beck, H. Electron-hole fluctuation phase in $1T$-$TiSe_2$. *Phys. Rev. B* **85**, 235150 (2012).

24. Bucher, B., Steiner, P. & Wachter, P. Excitonic insulator phase in $TmSe_{0.45}Te_{0.55}$. *Phys. Rev. Lett.* **67**, 2717 (1991).

25. Bronold, F. X. & Fehske, H. Possibility of an excitonic insulator at the semiconductor-semimetal transition. *Phys. Rev. B* **74**, 165107 (2006).

26. Di Salvo, F., Chen, C. H., Fleming, R., Waszczak, J. & Dunn, R. Physical and structural properties of the new layered compounds $Ta_2NiS_5$ and $Ta_2NiSe_5$. *Jour. of the Less-Comm. Met.* **116**, 51 (1986).

27. Okamura, Y. private communication (2014).

28. Wakisaka, Y. *et al.* Photoemission spectroscopy of $Ta_2NiSe_5$. *J. Supercond. Nov. Magn.* **25**, 1231 (2012).

29. Kaneko, T., Toriyama, T., Konishi, T. & Ohta, Y. Orthorombic-to-monoclinic phase transition of $Ta_2NiSe_5$ induced by the Bose-Einstein condensation of excitons. *Phys. Rev. B* **87**, 035121 (2013).

30. Zenker, B., Fehske, H., Beck, H., Monney, C. & Bishop, A. Chiral charge order in $1T$-$TiSe_2$: Importance of lattice degrees of freedom. *Phys. Rev. B* **88**, 075138 (2012).

31. Kaneko, T., Zenker, B., Fehske, H. & Ohta, Y. Competition between excitonic charge and spin density waves: Influence of electron-phonon and hund's rule couplings. *Phys. Rev. B* **92**, 115106 (2015).

32. Rohwer, T. *et al.* Collapse of long-range charge order tracked by time-resolved photoemission at high momenta. *Nature* **471**, 490 (2011).

33. Porer, M. *et al.* Non-thermal separation of electronic and structural orders in a persisting charge density wave. *Nature Mater.* **13**, 857 (2014).

34. See methods section for details.

35. Einstein, A. Die Quantentheorie der Strahlung. *Mitteilungen der Physikalischen Gesellschaft Zürich* **18**, 47–62 (1916).

36. Singer, A. *et al.* Photoinduced enhancement of the charge density wave amplitude. *Phys. Rev. Lett.* **177**, 056401 (2016).

## Acknowledgments

## Author contributions statement

C.M. and J.S. conceived the experiments; S.M., M.H. and C.M. conducted them; S.M., M.H., and J.S. analysed the data, D.G., P.W., and M. E. conceived and performed the calculations; S.M., M.H., C.M.,

D.G., P.W., M. E., and J.S. developed the interpretation of the results, N.K., M.N., H.T., and T.M. grew and provided the samples; S.M., C.M., D.G., and J.S. wrote the manuscript; all authors discussed and commented on the manuscript.
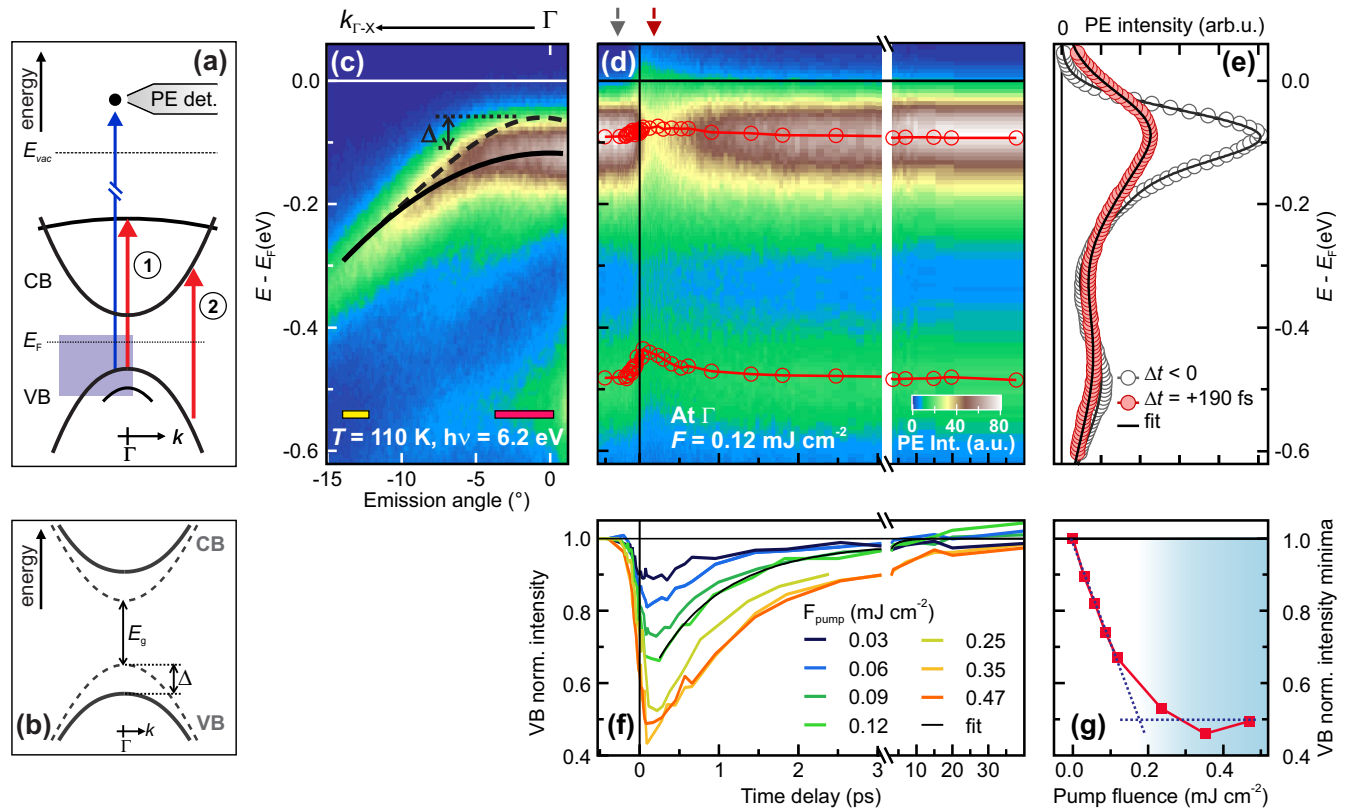
## Additional information

**Figure 1.** **(a)** Schematical band structure of $Ta_2NiSe_5$ at low-temperature. Electronic transitions induced by NIR optical excitation from the upper VB (red arrows) populate (1) a high energy empty $d$-band at $\Gamma$ or (2) the lower CB away near $\Gamma$. Time-delayed UV photons (blue arrow) are used to monitor the photoinduced changes to the occupied electronic structure by photoemission (blue shaded area). **(b)** Schematic EI (solid) and semiconductor (dashed) band structures. $E_g$ is the semiconductor band gap and $\Delta$ the enhancement of the gap related to the order parameter of the semiconductor-to-EI phase transition. **(c)** ARPES measurement of TNS at 110 K, showing the occupied electronic structure around $\Gamma$. **(d)** Transient changes of the PE intensity at $\Gamma$ as a function of the electron binding energy with respect to $E_F$ (left axis) and pump-probe time delay (bottom axis) at 110 K. Markers indicate the transient energetic position of the two VBs. **(e)** EDCs at equilibrium (empty grey circles) and 190 fs after photoexcitation (solid red circles). **(f)** Transient population of the upper VB at $\Gamma$. **(g)** Minima from (f) as a function of pump fluence: Below $F_C \approx 0.2$ mJ cm$^{-2}$, the VB population decreases linearly with excitation density, above the VB depopulation saturates at 50%. Dashed lines are linear fits.
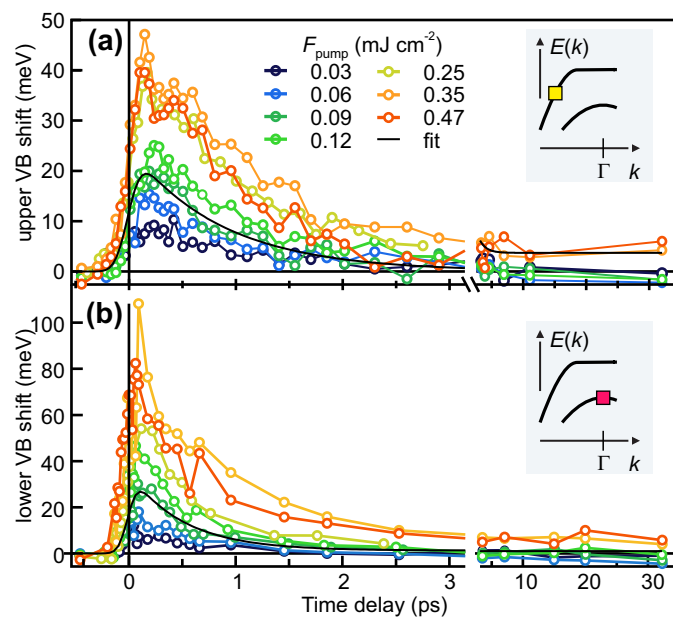
**Figure 2.** (a) Shift of the upper VB at $k \neq 0$ as a function of pump-probe time delay for different excitation densities. (b) Same analysis for the lower VB at $\Gamma$. Black lines in (a) and (b) are single exponential fits to the data.
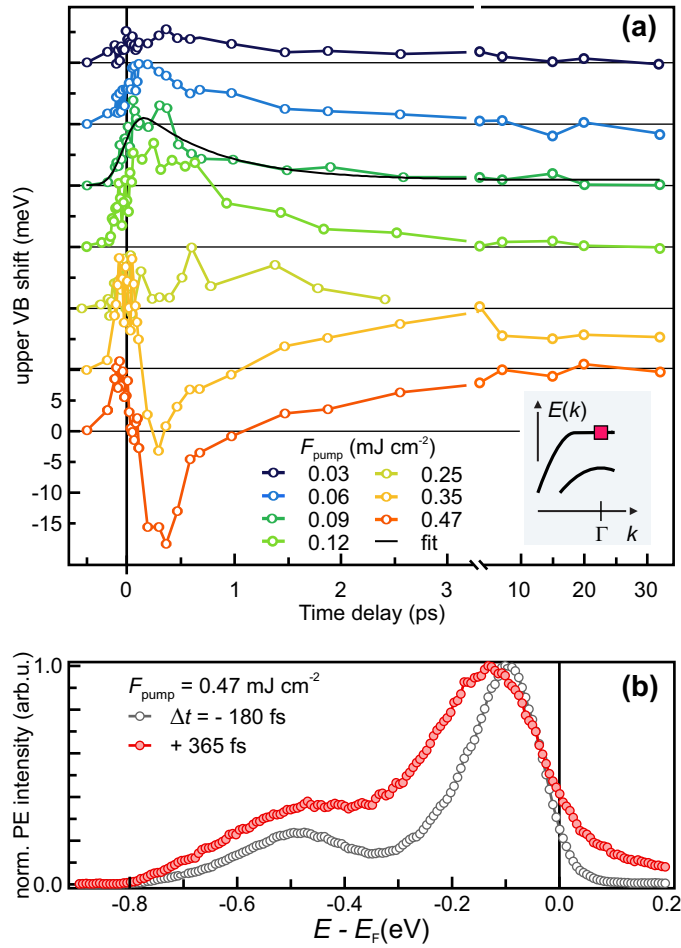
**Figure 3.** The shift of the upper VB at $\Gamma$ as a function of pump-probe time delay for different excitation densities (see text for details). **(b)** EDCs at $\Gamma$ before (empty grey circles) and 365 fs after (solid red circles) photoexcitation, when the upper VB transiently lies at higher binding energy than the equilibrium position.
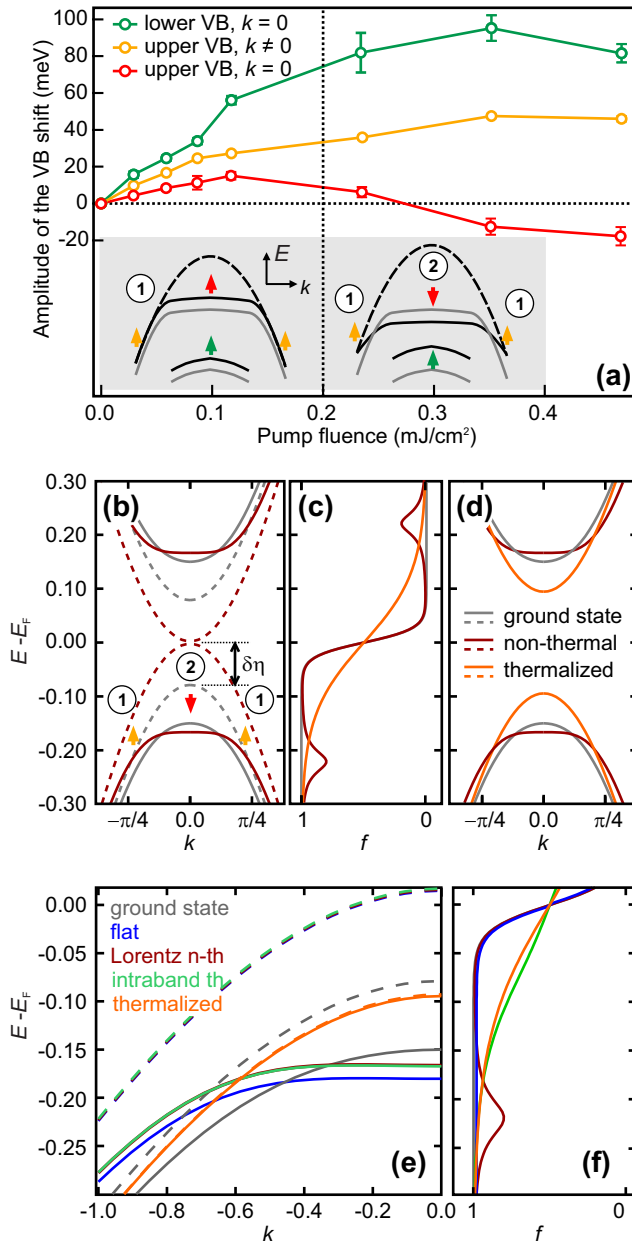
**Figure 4.** **(a)** The exponential fit amplitude of the shift of the lower VB at $\Gamma$ (green) and of the upper VB at $k \neq 0$ (yellow) as well as the amplitude of the shift at $\Gamma$ (red) as evaluated for a delay of 255 fs (see fig. 3(a)) as a function of the incident pump fluence. In the inset, the band structure dynamics are schematized for two excitation regimes, below (left) and above (right) $F_C$ respectively. **(b)** Dispersion relation for the initial ground state (grey) and a nonthermal distribution function (dark red), obtained from the Hartree-Fock calculations. The dashed lines show the bare semiconducting dispersion (with Hartree shift included). **(c)** Distribution functions corresponding to the dispersion relations in panel (b) and (d). **(d)** Comparison of the thermal state dispersion at the elevated temperature (orange) corresponding to the energy of the nonthermal state to the ground state and photoexcited nonthermal state. **(e)** Comparison of the ground state dispersion relation to the ones obtained from different nonthermal distribution functions, but with the same excitation density $n_{ex}$, namely in blue a constant population of holes (electrons), in dark red a dip (hump) in the Fermi-Dirac distribution function below (above) $E_F$, respectively, in green the corresponding *intra*band thermalized distribution at elevated temperatures. The negative energy parts of the corresponding distribution functions are presented in panel (f).